Article:
Pariota, L and Bifulco, GN (2015) Experimental evidence supporting simpler Action Point paradigms for car-following. Transportation Research Part F: Traffic Psychology and Behaviour, 35. pp. 1-15. ISSN: 1369-8478

https://doi.org/10.1016/j.trf.2015.08.002

1 Introduction

Modelling driving behaviour represents a crucial task for many applications in transportation. Three main areas can particularly benefit from an enhanced knowledge of driving behaviour: accident analysis and prevention, microscopic simulation of traffic, and Intelligent Transportation Systems (ITS). Benefits for ITS are mainly expected in the field of Advanced Driver Assistance Systems (ADAS), where some assistance/control logics interact with drivers (and their behaviour) and where both drivers' expectations, and impacts of the innovations on drivers' behaviour have to be considered in order to improve: a) the effectiveness of the solutions; b) driving (and traffic) safety and c) acceptance of technological solutions.

Modelling of driving behaviour is based on two fundamental requirements. On the one hand, theoretical frameworks and paradigms are needed. On the other, observation tools and data are required in order both to develop/validate theories and to identify modelling parameters for practical applications. If the research focus is on disaggregate driving behaviour rather than aggregate traffic behaviour, the best source of information is based on individual vehicle data (IVD), as typically obtained by instrumented vehicles (IVs). An IV can be described as a standard vehicle where the kinematics, the interaction with surrounding vehicles and the vehicle-driver interaction are recorded for subsequent analysis. The possibility of observing only the kinematics of IVs, as allowed by some camera-based microscopic roadside observation systems like in the NGSIM project (Alexiadis et al., 2004), can lead to a reduced understanding of driving behaviour. Indeed, the possibility of observing the kinematics of an IV is just a prerequisite and IVs are usually equipped with a large number of sensors. Multisensing approaches not only enhance the estimation of the *ego-kinematics* of the controlled vehicle (Bifulco et al., 2011), but also allow detection of the surrounding traffic conditions and direct monitoring of on-board interaction between the driver and the vehicle, generally via the controlled area network (CAN). The overall result is a more comprehensive observation and enhanced understanding of driving behaviour.

Different aspects of driving behaviour can be analysed thanks to the data collected by means of IVs. At least two of these aspects are relevant to the field of ADAS: the longitudinal and lateral control of the vehicle. Lateral control involves manoeuvres such as lane keeping, lane changing and overtaking. In the case of longitudinal control, various conditions are often considered, such as free flow, approaching, car-following, emergency braking, and stop and go. Of these, the car-following process has probably been the most extensively studied.

Car-following models estimate the kinematics of a following vehicle as a response to the stimuli of a leading one. These paradigms assume that the follower adapts his/her speed to the vehicle ahead. Though some models have been proposed with a look-ahead approach, that is, based on the influence of more than one vehicle in the leading platoon (see Hoogendoorn and Ossen, 2006, for an empirical analysis), most approaches assume that the phenomenon can be mainly explained in terms of the vehicle directly ahead. In practice, in these models, each update of the follower's kinematics is obtained by considering its instantaneous position, and the speed and some kinematic variables of the leader. An exhaustive review of car-following models lies beyond the scope of this work and can be found in Saifuzzaman and Zheng (2014). According to this review, car-following paradigms can be classified, depending on their basic approach, in *Engineering* models and *psycho-physical* paradigms. This is a not new classification that Saifuzzaman and Zheng argument and develop, and that is perhaps the most widely accepted in the scientific literature.

Engineering car-following models apply Newtonian laws of motion to approximate car-following behaviors. The most studied model in this stream is probably the *stimulus-response* model by Gazis et al. (1961),

developed at the General Motors labs in Detroit. Several other relevant approaches are the *safety-distance* model of Gipps (1981), or the *desired measures* model proposed by Treiber et al. (2000). Other approaches have emerged from the applications into the car-following behaviour studies of bio-inspired artificial intelligence concepts such as Artificial Neural Networks (Colombaroni and Fusco, 2014), fuzzy-logic (Kikuchi and Chakroborty, 1992) or cellular automata (Bham and Benekohal, 2004).

Models based on *psycho-physical* paradigms have been developed from human-factors studies. They move from the assumption that *Engineering* models are unable to characterize the process of human thinking (and solving) associated to the *driving problem*. As well addressed also in Saifuzzaman and Zheng, even if several attempts to embed human behaviours into *Engineering* models have been carried out (recently Pariota et al., 2015 on-line publication), *psycho-physical* paradigms are characterised by quite peculiar (and convincing) fundamental assumptions on the human behaviour. As an example, drivers are assumed to adopt a satisficing performance evaluation strategy, rather than an optimal one (Boer, 1999), that means humans are often incapable of identifying and implementing optimal control strategy (Zgonnikov and Lubashevsky, 2014); moreover, are they can be observed to do not apply a continuous control (Wagner, 2011).

All the previous does not prevent from arguing that the *stimulus-response* and/or the *fuzzy-set* (or some other) approaches can also be considered to have a psycho-physical nature and both pros and cons can be debated on this point. However, this is mainly a definitional point, which arises from the attempt to give an ordered classification of the proposed models. Moreover, it should be clearly stated that cases could exist whose basic assumptions can blur. For example it could be proved that stimulus reaction model by Michaels (1963) that will be presented later (as a *psycho-physical* paradigm) is equivalent to the formulation of GHR model with sensitivity proportional to the inverse square of spacing, which leads to the Greenshields model in a stationary traffic state (Saifuzzaman and Zheng, 2014).

Within psycho-physical models, the action point (AP) approach seeks to describe the behaviour of a follower with respect to several thresholds, applied to the perception of different influencing stimuli coming from the leader. The AP paradigm has also been applied to microscopic traffic modelling (e.g. VISSIM), inspiring several researchers (Hoogendoorn et al., 2011). Recently, Bifulco et al. (2013) took a step forward in exploiting AP theory in the field of ADAS with the introduction of the *car-following waves* concept.

The most widely used formulation of AP theory was proposed by Wiedemann (1974), even if earlier (and simpler) approaches were proposed by Barbosa (1961) and Todosoiev (1963). The latter models are introduced in section 2, where Wiedemann's theory is shown to be more general but more complex, as it requires identification of two further AP thresholds. Some experimental evidence is analysed in order to investigate the proposed approaches under a new light and identify a good trade-off between their generality, robustness and simplicity. Section 3 presents the experimental campaign in which data were collected, carried out during the Italian DriveIN^2 research project (Bifulco et al., 2012). Data are first of all analysed in terms of *kinematically*-identified APs (as in Brackstone et al., 2002), and then validated versus observed actual drivers' actions. The discussion of the results allows some appropriate conclusions to be drawn, the most important being that that in the great part of the cases (at least among those observed in the DriveIN^2 campaign) it is worth adopting a simpler approach. This results confirm, by using a different kind of analyses (actions on pedals) and a different dataset, the ones obtained in Bifulco et al. (2013), where only kinematic observations were adopted. Another main contribution of this paper is to propose to ascertain from candidate APs and actual ones. Moreover, the carried out analyses are based on a (much) more extended naturalistic (road) survey experiment with respect to Bifulco et al. (2013), as well as on the

exploitation of additional data collected by means of two different kinds of driving simulators. It is also worth noting that the new framework proposed by this paper allows for analysing the time distribution of drivers' actions, as well as to reciprocally confirm observations from road and virtual driving experiments.

2 Action point paradigms

In the early work by Michaels (1963), it is argued that the stimulus to which drivers respond is the angular velocity (d□ / dt) at which the *apparent size* of the vehicle ahead changes, where the apparent size is defined as the visual angle (□) subtended by the observed leading vehicle.

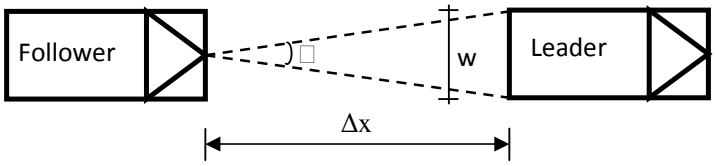

The angular velocity is proportional to both the current relative speed ($\Delta v^t = v_L^t - v_F^t$, where v_L^t and v_F^t are the current speeds of the leader and of the follower) and the spacing (Δx^t), via equation 1 below:

$$\frac{d\theta}{dt} = -w\frac{\Delta v^t}{(\Delta x^t)^2} \qquad 1)$$

The angular velocity should be non-negligible in order to stimulate the driver of the following vehicle and induce action. An example of the argued role of the angular velocity can be given with reference to the transition from a free-flow to an approaching condition. In free-flow the follower is actually approaching a (slower) leading vehicle from far away, but does not yet realize that he/she is in an approaching condition. Indeed, the following vehicle is at a distance greater than that at which any variation of the angular velocity can be detected; in other terms, according to equation 1, Δx^t is so large that d□ / dt proves negligible. As the distance progressively decreases, the angular velocity attains a non-negligible value which can be perceived by the driver, who starts adapting his/her cruising speed with respect to the leading vehicle (actual approaching phase). This point where the change of the visual angle starts to be perceived is identified in Michaels' theory at a value of about $6 \times 10^{-4}\, rad/sec$. According to Michaels' theory, once this threshold is exceeded and the driver approaches the leader by decelerating, the angular speed slows down, the driver tends to close on the leading vehicle, and finally he/she tends to both a relative velocity close to zero and a separation that still allows steering control and the viewing/safety distance to be maintained. This is the steady-state condition where, should the drivers have perfect control over their vehicles, the leader-follower pairs proceed with constant headway and constant spacing (the relative speed being null). However, it is more likely that in this condition the drivers are unable to fully control the acceleration/deceleration of their vehicle, due to the excessively fine adjustments required. Thus the dynamics of the vehicle is governed by small values of acceleration and deceleration, as in Montroll's acceleration-noise concept (Montroll, 1959): the relative speed oscillates around the null value and the spacing around the desired value. These small fluctuations come from the acceleration/deceleration applied by the driver as a response to the stimuli perceived once two significant values (thresholds, of opposite sign) of the angular velocity are reached. According to equation 1, when the relative speed and the spacing are such that the angular velocity is not perceived (below the threshold, in absolute value) drivers retain their current behaviour. Rather, they accelerate if the angular velocity reaches the negative threshold and decelerate when the angular velocity reaches the positive threshold. The modelling framework assumes that the acceleration is kept constant from one threshold to the other.

Other research has been carried out to identify conditions and thresholds that determine drivers' actions in car-following. Mention should be made of the investigations carried out by Barbosa (1961) and Todosoiev (1963) through the use of driving simulators, employed at their very early technological stage. Barbosa started to study car-following behaviour by means of so-called *phase plane* trajectories. Given a dynamic system, a *phase plane* is a Cartesian plane in which states (or phases) of the physical system are mapped; in common use, a characteristic state of the system is plotted together with its time-first-derivative. Barbosa having chosen spacing as the characteristic state, the phase trajectory (or *phase portrait*) was identified by spacing (x axis) and relative speed (y-axis). The phase portrait resulting from observed car-following data gives rise to the well-known *car-following spirals* used extensively by analysts. Barbosa interpreted the trajectories as very close to being parabolic (as depicted in Figure 1 below, left). This paradigm is consistent with Michaels' theory, as it implies that the second derivative of the spacing is piecewise constant with respect to the relative speed. It coincides, assuming constant acceleration of the leading vehicle, with the opposite of the follower's acceleration; hence the follower's acceleration is (piecewise) constant. According to this paradigm, Barbosa proposed the *decision-point* model, defining the points where the driver makes decisions to accelerate/decelerate at a constant acceleration/deceleration rate. The overall result of Barbosa's approach is a trajectory that oscillates around the equilibrium points (null relative speed and desired spacing, according to Michaels).

Place Figure 1 about here

These studies inspired Todosoiev (1963), who analysed the car-following process in the relative acceleration vs. relative speed plane, which he defined, consistently with Barbosa, as the *second-order phase plane*. As already stated, parabolic trajectories obtained with the model proposed by Barbosa correspond to rectangular trajectories in the second-order phase plane. It is worth noting that the trajectories abruptly change sign (from constant deceleration to constant acceleration and vice versa, with infinite jerk). These discontinuity points are evident in Figure 1 (right); Todosoiev was the first analyst who called them *action points* (APs) and the associated model the *Action-Point Model*.

After the analyses by Todosoiev, Wiedemann (1974) established his own (well-known) action-point paradigm. The theory by Wiedemann is more articulated (and complex). He introduced a formalism able to distinguish between different longitudinal driving conditions: a vehicle not influenced by any front vehicle; consciously influenced because the driver perceives a slower vehicle ahead; unconsciously influenced by the vehicle ahead and in steady-state car-following (*close-following*) conditions; in emergency situations. Wiedemann developed the framework for dealing with the transition between these different conditions on the basis of appropriate thresholds. In practice, in Weidemann's scheme, as shown in Figure 2 below, the follower drives uninfluenced until the SDV threshold is reached; then the driver consciously starts to decelerate because of the perceived slower vehicle. According to Michaels' scheme, he/she tries to maintain a certain headway and a null relative speed, but, unconsciously, he/she oscillates between the four thresholds, namely CLDV, ABX, OPDV and SDX, that define the close-following condition in terms of spacing and relative speed. In this condition each time a stimulus is perceived, the driver applies a constant value of acceleration, and holds this value until a new stimulus is perceived. The absolute value of the acceleration applied was parameterized by Wiedemann with a parameter called *bnull,* which has the magnitude of Montroll's Noise (Montroll, 1959), while the sign of the acceleration is negative or positive consistent with closing or opening intentions. The driver behaves in this way indefinitely unless an external change (e.g. emergency braking or sudden acceleration of the leader) occurs.

Place Figure 2 about here

Wiedemann's theory is summarised in Table I, where the expected kinematics and actions at each AP are made explicit. Importantly, the paradigm can still be interpreted with the help of equation 1 which identifies the angular velocity. It is evident that the (four) Wiedemann thresholds include those (two) of Barbosa and Todosoiev, where we can assume that only OPDV and CLDV points are considered since, according to Table I below, only changes from deceleration to acceleration are taken into account (also compare Figure 2 and Figure 1-left, after considering the Cartesian axes are rotated).

Place Table I about here

Importantly, the same multi-regime approach argued by Wiedemann can be found in other versions of the AP paradigm. Amongst others, it is worth citing Fritzsche (1994) who used different thresholds (with different formulations for them) to describe the longitudinal driving behaviour as a combination of behaviours performed in different regions. Again, a *bnull* value of acceleration is used, equal to 0.2 m/s^2, to model the inadequacy of the driver to fully control the vehicle. Another model was proposed by Fancher and Bareket (1998); it is action-point-like, but assumes the perception thresholds for relative speed as evaluable by using the *looming effect* theory. From this study some information about the first threshold described in the Michaels model was obtained. Indeed, also using results from Hoffmann and Mortimer (1996), they evaluated a perception limit for $\frac{d\theta}{dt}$ of about $3 \times 10^{-3}\, rad/sec$ (5 times bigger than those given in Michaels).

It is generally difficult to prove or refuse the validity of all different proposed Action-Point models, since experiments related to the calibration of the thresholds are difficult to carry out. Nevertheless, the hypotheses all these paradigms are built upon seem realistic. The aim of this paper with respect to the current state of the art is to clarify the role played by the thresholds for either relative speed or spacing. We seek to ascertain the actual need of more simple or complex approaches towards AP theory. Using experimental evidence we support the choice between Wiedemann's approach and the more simplified approaches adopted by Barbosa and Todosoiev, paving the way for more effective calibration of the required thresholds.

3 Testing Action Point paradigms

3.1 Collection of experimental data

Our tests were carried out on data collected in the framework of the DriveIN[2] research project (Bifulco et al., 2012). The project involves eight partners (including Fiat Chrysler Automobiles, the major Italian car-maker) and focuses on defining methodologies, technologies and solutions aimed at capturing driving behaviors using different experimental environments.

For this project an extensive experimental campaign started in September 2012 has been adopted. The campaign comprises 100 driving experiment. An initial pool of 150 participants took part in the study, having responded to advertisements requesting volunteers for a study on driving behaviour. A sample of

100 participants was drawn from this pool to match the population of Italian drivers with respect to gender, age and educational level.

Each driving experiment consisted of (at least) two driving sessions, one on the road and one in a static driving simulator (S-DS) environment; 22 (randomly selected) drivers also drove a dynamic driving simulator (D-DS). Both on the road and in the virtual environments the drivers drove across the same driving scenario. It comprised a single loop on three roads near Naples: (1) National Highway A1 (14 km), consisting of a dual carriageway and three lanes of traffic in each direction, a design speed interval of 80-120km/h (speed limit 100 km/h); (2) National Highway A30 (30 km), with characteristics similar to National Highway A1, but with a posted speed limit of 130 km/h; (3) Rural Roadway SS 268 “del Vesuvio” (16 km), with a single carriageway with one lane in each direction, at-grade intersections and a design speed interval of 60-80 km/h. The three sections were preceded by a 10 km acclimatization section and followed by an 8 km urban path to close the loop. In all, the loop was 78 km long. Each driving session lasted about 1 hour. At driving simulator the driving session was inclusive of an additional 10-min short practice, that was carried out to become familiar with the simulator. The experimental campaign lasted two months and was carried out in daily experimental sessions, each consisting of a few (up to 5) driving sessions.

The on-road driving sessions were carried out by means of the instrumented vehicle (IV) owned by the University of Naples. It is equipped with systems (inertial measurement sensors, GPS, sensors on pedals and steering wheel, connection to the on-board CAN, forward and backward radars, and video cameras) designed to monitor the driver’s actions, the resulting vehicle kinematics and the surrounding vehicles.

The S-DS consists of a single-seat cockpit, with all the driver controls. A real-time anti-aliased 3-D graphical scene of the virtual world is visualized on three surrounding 23" monitors at a total resolution of 5040 x 1050 pixels. The total horizontal and vertical fields of view are 100° and 20°, respectively. The frame rate is constant and fixed at 60Hz. The driving experience provided by the static simulator is enhanced by a surround sound system that simulated the various sound sources (e.g. engine, wind, tyres, etc.). Although the simulator is fixed-base, torque feedback at the steering wheel is provided and adjustable springs provide all the pedals with realistic force feedback.

The D-DS uses three flat wall-screens (3.00m×4.00m) that surround the motion platform. The visual scene is projected to a high-resolution three channel 180 × 50 forward field of view with rear and side mirror views replaced by 6.5” LCD monitors. The visual system allows a resolution of 1400×1050 for each channel and a refresh rate of 60 Hz. The cockpit is one half of a real Citroen C2 with two adjustable seats and a real equipped dashboard. The audio system can reproduce various sounds that can normally be heard while driving. Feedback is provided by a force feedback system (SENSO-Wheel SD-LC) on the steering and a six degree-of-freedom electric motion platform. Torque feedback at the steering wheel is provided via a motor fixed at the end of the steering column. The motion system consists of a Cuesim hexapod with six electric actuators, able to reproduce the accelerations that real car occupants feel.

Importantly, during the whole road experimental campaign weather conditions did not differ substantially across driving sessions; moreover, on-road experiments were carried out only in work-days in order to allow for homogeneous traffic conditions. In particular, unsaturated traffic conditions were always observed, without stop and go phenomena. A negligible percentage of trucks was always encountered on the two motorways, while for the rural roadway a percentage of trucks ranging from 15 to 20 % was observed. The different type of leading vehicle could possibly bind the behaviour of the drivers (e.g. in the choice of adopted headway). With reference to the focus of this paper we retain that the different size of the leading vehicle could have mostly an effect on the value of the reaction-thresholds, than on the behaviour of the drivers once the thresholds are reached; thus our analyses do not take into account this

variable. Note that both the driving simulators were provided with a traffic-simulation module, allowing for the emulation of traffic conditions according to the desired average speed of the traffic stream and traffic density. These parameters were tuned in order to adapt the simulated experimental conditions to the prevailing ones on the road. Many other information on the sample, the total data collected, and the results of DriveIn[2] project can be found in Bifulco et al. (2013).

The large amount of data collected is used to search for evidence on the action actually taken at (candidate) action points, according to expected actions identified in the last column of Table I above.

3.2 Identification of candidate Action Points

Before analyzing APs, collected data have undergone several pre-process steps. In the first step each trajectory observed for each driver has been split in several *sections*. Each section is characterized by a unique leading vehicle and by uninterrupted car-following conditions. As a result of the trajectory sectioning, non-car-following conditions are discarded. The process is carried out by by means of a manually-made visual analysis of the video taken by the front camera of the IV. In the two simulators the step is made easier because the relative positions of all the vehicles in the simulation are known. All the AP analyses have then been applied to the sections.

Collected data allow car-following spirals to be plotted in the phase-plane, as well as action points (APs), defined according to Wiedemann's theory. An example is depicted in Figure 3 below (left) for few seconds of observation.

The procedure for AP identification was taken from Brackstone et al. (2002); similar procedures have been proposed by other authors (Wagner, 2011; Hoogendorn et al., 2011). All these techniques base identification of APs on kinematic conditions; identification of these points is straightforward if one analyse trajectories in the phase-plane (as in Figure 3 left side). When adopting the procedure, we did not employ any filter neither on the follower's speed nor on the length of the spirals. Using the chosen technique, we selected four types of APs (CLDV, OPDV, ABX, SDX), according to Wiedemann's theory.

Place Figure 3 about here

The previous *kinematically*-identified APs are here viewed as *candidate action points*; they have to be confirmed as *actual* APs by searching for actual actions (on pedals) made by the driver in a time-window around the time of detection (t_{ap}) of the candidate AP. Indeed, the time window searched for the actual actions is extended before t_{ap}, as the observed kinematic variation is the effect of an action which, given the powertrain and other vehicle inertia, should have started before. Moreover, drivers' actions could also hold over t_{ap}, as the latest is just the instant when the effect of the action is identified for the first time. As a consequence, each time a point is detected as a candidate AP, the trajectory of observed variables are associated to t_{ap} for all instants within a predetermined range. The considered range is [t_{ap} -3, t_{ap} +3], as three seconds is arbitrarily hypothesised as a time-window to which both the start and the end of the action belong for sure. This hypothesis will be confirmed below. Recorded variables are the speed and the acceleration of both the leader and the follower, as well as the inter-vehicular spacing and, last but not the least, the values of the pedals (gas and brake) pressure. The number of drivers for each environment (static and dynamic driving simulator, and instrumented vehicle), information about the selected sections, as well as the number of detected candidate APs are shown in Table II.

Place Table II about here

Given the huge quantity of data, an efficient way to analyse and represent them has to be identified. It was thus chosen to analyse the data in an aggregate way; this is consistent with our aim to highlight the most frequent driving behaviours. Hence we refer below to statistical distributions of relevant variables (e.g. actions on pedals) observed over the experimental dataset as a whole. Moreover, we often represent the data by appropriate box-and-whisker plots. In principle, the actual action searched for at candidate APs is any variation in pedal pressure, since the gas pedal and brake are the actuators that the driver is expected to control once in a car-following situation. We argue below in favour of analysing the gas-pedal alone.

Our analyses refer to the instrumented vehicle, provided that scenarios based on virtual reality could be questioned with respect to the realism of the observed driving behaviours. However, we exploit the availability of observations collected at driving simulators in order to qualitatively confirm the results, once identified on the instrumented vehicle. It is worth noting that the data observed at the driving simulators are expected to present a narrow dispersion and a sharper pattern, as they are unaffected by real-word biases.

3.3 Identification of actual Action Points

During car-following drivers control their vehicles by mainly using the gas pedal and, to a lesser extent, the brake. The latter pedal is more likely to be employed in emergency-braking conditions, as slow decelerations generally required in car-following conditions can often be applied by simply relaxing the gas pedal. In our data, given the experimental conditions (suburban close-following and approaching conditions, without stop-and-go phenomena) and according to both expectations and previous studies (e.g. Bifulco et al., 2013), we found that the use of the brake pedal is rare. Indeed, the number of times when the pressure on the brake pedal exceeded 1% represents about 7% of the total observations. Of course, as long as we have observed close-following conditions, collected acceleration are almost all in the range -1.5/1.5 m/s^2, that is consistent with expectations in our experimental conditions.

Our analyses will search for actual actions starting from the definition of the gas-pedal pressure $\gamma\gamma(t)$; this represents the instantaneous value of pressure the driver applies to the accelerator; this varies from 0 (pedal fully-relaxed) to 1 (pedal fully pushed down). From $\gamma(t)$ we measure:

- the *relative gas pedal pressure*, $\gamma_r(t) = \gamma(t) - \gamma(t_{ap})$; this represents the difference between the instantaneous value of pressure the driver applies and the value of pressure applied in the instant t_{ap} of candidate AP detection; it varies from -1 to 1;
- *variation in gas pedal pressure*, $\Delta\gamma_r(t)= \gamma_r(t+\Delta t)- \gamma_r(t)$; given that the sampling step of our data collection is $\Delta t=0.1$ seconds, the variation is proportional (with a 10 coefficient) to the numerical derivative of the pedal pressure.

Place Figure 4 about here

An example of the value assumed by variables γ_r and $\Delta\gamma_r$ in one manoeuvre (arbitrarily chosen) is represented in Figure 4 . Note that the action is all within the range of analysis [t_{ap} -3, t_{ap} +3] and that choosing t_{ap} as the reference time seems to be an appropriate hypothesis.

The statistical analyses of the observed $\gamma_r(t)$ trajectories for the four different types of candidate APs (CLDV, OPDV, ABX, SDX) are shown in Figure 5 below. Note that adopting $\gamma_r(t)$ instead of $\gamma(t)$ allows normalising with respect to the absolute magnitude of the applied acceleration/deceleration, which may differ greatly for different detected candidate APs. For the sake of visual clarity, plots are shown with reference to sub-sampling with 0.6-second steps in the time-interval [t_{ap} -3, t_{ap} +3]. The representation makes use of box and whisker plots; boxes represents the 25^{th}, 50^{th} and 75^{th} percentiles and whiskers cover 95% of the distributions.

Place Figure 5 about here

In Figure 5 we search for characteristic patterns of the gas pedal as expected at the different types of APs and in accordance with the rightmost column of Table I above. In order to interpreter the figures shown by the charts above, just as an example, please refer your attention to the upper-left chart. Note that in 75% of the cases the value assumed by γ_r 3 seconds before to the instant t_{ap} is positive, moreover, in 50% of the cases it is greater than 0.05 and in 25% of the cases it is greater than 0.10. These values are remarkable if one takes into account two things: i) the average value of γ observed in the same instants with reference to CLDV points (computed across all considered trajectories) is around 0.15, with a standard deviation of 0.1; the average value of γ observed at t_{ap} with reference to CLDV points (computed across all considered trajectories) is around 0.08, with a standard deviation of 0.07. Thus a value of about 0.05 for γ_r represents a relevant quantity for the phenomenon. Similar considerations can be made can be made also with reference to the other candidate APs. With reference to values depicted in Figure 5, the Standard Error of the Mean (SEM) has been computed for each of the boxes. Computed SEM values range (for all the boxes, and for all the candidate APs) in the interval [0-0.0019] (it should be noted that for normal distributions the Standard Error of the Median is about 25% larger of the SEM); the values assumed by the SEM confirm that results showed in Figure 5 (e.g. median values of γ_r) are very significant.

The expected reduction of γ_r is clearly observable at the CLDVs, as well as the expected increment at the OPDVs. The driver relaxes the gas pedal when he/she realizes that the gap is closing too much, while on the other hand he/she increases the pedal pressure when he/she realizes that the gap is opening too much. Interestingly, CLDVs and OPDVs are detected (by kinematic conditions) once the action has been completed, and the pedal pressure has become nearly constant. Unlike expectations made explicit by Table I in section 2, two *flat zones* are exhibited before the detection of candidate ABX and SDX points. In particular before the time instant t_{ap} the two distributions persist around the null value. It is worth noting that for ABX points a slight increment of γ_r after t_{ap} is observed; this is counterintuitive and in contrast with the expected action described in Table I (a further relaxing of the gas pedal). The same, in the opposite manner, happens after t_{ap} for SDX points (a slight relaxation of the gas pedal instead of an expected further pressure (Table I). The counterintuitive results can be explained considering that for each spiral ABX precedes OPDV, and SDX precedes CLDV. Indeed, given the large time of observation after t_{ap}, it would be logical to think that the above unintuitive behaviour is an effect of the actions associated to the forthcoming OPDVs and CLDVs, and not a matter of actions associated to ABXs and SDXs. This suggests that the actual interval in which the action can be analysed is narrower than [t_{ap} -3, t_{ap} +3]; this will be confirmed by some further analyses below.

That said, the behaviour at candidate points ABX and SDX seems to contradict Wiedemann's approach. The absence of significant actions before ABX and SDX confirms the early theories by Barbosa and Todosoiev. Alternatively (and not contradictorily), a particular case of Wiedemann's paradigm could have occurred, as described by Figure 6 below, where the thresholds for ABX and SDX lie outside the region identified by the natural slope of the spiral determined by the actions performed in OPDV and CLDV. In this case, it is possible (from a purely kinematic point of view) to identify some F_SDX (*False SDX*) and F_ABX (*False ABX*) points, as these are the points where the gradient of the spacing becomes null. However, these points do not correspond to any actual action and are only the direct consequence of actions previously taken at OPDV or CLDV.

Place Figure 6 about here

The aggregate analysis in Figure 5 suggests that the particular case of Wiedemann's theory illustrated in Figure 6 is very likely to hold (at least in the observed dataset) and that the thresholds for ABX and SDX almost never bind actual driving behaviour.

An aggregate analysis of the $\Delta\gamma_r(t_{ap})$ values is shown in Figure 7 below, where the distributions of the median values of $\Delta\gamma_r(t_{ap})$ at the four candidate types of APs are plotted. They confirm the results of Figure 5 and hence the interpretation that the most likely conditions are those identified by the particular case of the Wiedemann paradigm. Variations in gas pedal pressure are mainly observed around points CLDV and OPDV, while they are negligible before ABX and SDX. Figure 7 also allows better identification of the actual range around t_{ap} where much of the action can be revealed. This range seems to be no more extended than 1.6 seconds before and after t_{ap}.

Place Figure 7 about here

The previous analyses can be validated by also looking at the acceleration and deceleration patterns. To this end, we use the following terms:

- the instantaneous follower's acceleration, $\alpha(t)$: this represents the instantaneous value of the detected acceleration;
- the instantaneous relative follower's acceleration, $\alpha_r(t) = \alpha(t) - \alpha(t_{ap})$: this represents the difference between the instantaneous value of the detected acceleration and the value detected in the instant t_{ap}, where the candidate AP has been identified.

The observed relative follower accelerations are shown in Figure 8 below, where the interval of 1.6 second before and after the candidate AP was adopted as a consequence of the lesson learned from Figure 7.

Place Figure 8 about here

Note that the transition from acceleration to deceleration is evident at CLDV and vice versa from deceleration to acceleration at OPDV. Once again, a flat zone is revealed at ABDX and SDX, instead of respectively the expected (see the third column in Table I in section 2) further deceleration and further

acceleration. From the quantitative point of view, Figure 8 shows that the decrease at CDLV and OPDV is (for the median values) about 0.2 m/s^2 (the acceleration turns from 0 to about -0.2 m/s^2 at CLDVs and from about -0.05 m/s^2 to 0.15 m/s^2 at OPDVs).

It is interesting to test the sensitivity of our results with respect to the value of $\alpha(t)$. To this aim we have repeated our analyses after having defined a cut-off value on $\alpha(t)$, so far not employed. the cut-off value is the maximum value admitted in our analyses in order to consider the observed manoeuvre actually belongs to the Wiedemann's *unconscious reaction zone*. Greater values could correspond to other phenomena such as emergency braking or sudden leader's accelerations. For different cut-off values a different number of manoeuvres has been discarded from the analysis. Given that the appropriate cut-off value is unknown, a parametric analysis has been done. The used cut-offs have been: none, 1.5, 1.25, 1, 0.75 and 0.5 m/s^2. Of course if no cut-off value is applied, then any observed manoeuvre is considered as consistent with the AP theory, on the other hand the cut-off value of 0.5 m/s^2 bounds the AP area probably in a too narrow way. As can be seen by Figure 9, the observed behaviour is such that even a small cut-off value (e.g. 1 m/s^2) allows us to consider more than 80% of the dataset as representative of the behaviours in the *unconscious reaction zone*.

Place Figure 9 about here

However the trends around APs observed in Figure 8 are not affected by the selected threshold, nor are affected the $\alpha_r(t)$ reached values if reasonable cut-off values (not less than 1 m/s^2) are considered. This can be seen in Figure 10 where the median values of $\alpha_r(t)$ for all the cut-offs have been reported.

Place Figure 10 about here

Finally, data in the Figure 8 are also confirmed at the simulator, where much of the bias that affects the IV data is eliminated. The results are much more evident than in the case of the IV and are shown in Figure 11 below (the left side refers to the static simulator and the right to the dynamic simulator).

Place Figure 11 about here

The flat zone at points ABX and SDX is particularly evident, while respectively a decrease and an increase of the acceleration is observed at points CDLV and OPDV. In quantitative terms, with respect to points CLDV, the median value of $\alpha_r(t)$ decreases from 0.1 m/s^2 to -0.5 m/s^2 (thus the total deceleration is about -0.6 m/s^2) at the static simulator, while in the dynamic simulator it decreases from 0.15 m/s^2 to -0.2 m/s^2 (thus with a total variation of about 0.35 m/s^2); with reference to points OPDV the median value of $\alpha_r(t)$ increases from -0.1 m/s^2 to 0.25 m/s^2 (thus the total acceleration is about 0.35 m/s^2) at the static simulator, while in the dynamic simulator it increases from -0.1 m/s^2 to 0.1 m/s^2 (hence with a total variation of about 0.2 m/s^2). The dynamic simulator seems to lie half way between the instrumented vehicle and the static simulator, thus suggesting that, as expected, a more realistic virtual environment is a better proxy of the real world.

3.4 Analysis of driving behaviour at action points

Detection of consistent patterns at CLDVs and OPDVs helps to quantify some characteristics related to manoeuvres at them. In particular, the time interval in which $\Delta\gamma_r(t)$ has a significant value coincides with the time interval in which the action is actually performed. Figure 12 below again shows the plots over time for the median of $\Delta\gamma_r(t)$, adding that revealed at the two virtual environments (and restricting the analysis in the range of 1.6 seconds before and after the identified AP time, when all the actions occur in all environments).

Place Figure 12 about here

Much additional information can be drawn. The patterns observed in the different experimental environments are all similar, and are consistent with expected behaviour. Notably, the durations of closing and opening manoeuvres are quite different. These differences can be discussed with respect to two levels.

At a first level, with reference to median values, actions related to CLDV points last 1.6 seconds in the S-DS, and range from 1.2 seconds before to 0.4 seconds after t_{ap}. In the D-DS the previous time window is shorter (1 second); the actions start later (0.6 seconds before t_{ap}), and finish at the same time (0.4 seconds after t_{ap}). The IV data show a situation which is more similar to the S-DS (the time window is again 1.6 seconds), although actions start, and finish, 0.2 seconds later (respectively at t_{ap} -1, and t_{ap} +0.6). A similar trend is observed also with respect to OPDV data. Two comparable time windows are observed again for the S-DS and IV data: manoeuvres start at t_{ap} -0.8 and t_{ap} -1.2 seconds, and stop at t_{ap} +1.6 and t_{ap} +1.2 seconds, respectively. A shorter time window is observed in the D-DS environment (actions start at t_{ap} -0.6 and t_{ap} +1 seconds). Consistently for all the experimental environments, actions around OPDV points last longer, and the instantaneous variations of $\gamma_r(t)$ are smaller around OPDV points compared to CLDV points.

Another major point concerns the actual variation of gas pedal pressure ($\Delta\gamma_r$) in the three environments. The variation is chosen as it normalise the analysis from the absolute value of the pressure that has no actual behavioural meaning, as it depends on the actual sensitivity of the pedal, on the engine and on the powertrain, and typically differs from vehicle to vehicle, and from real vehicle to driving simulator. It has to be noted that the data of $\Delta\gamma_r$ for the IV are more similar to those for S-DS. They range in the interval $-0.003 < \Delta\gamma_r(t) < 0.003$ for the IV, and in the interval $-0.010 < \Delta\gamma_r(t) < 0.005$ for S-DS, while they have a greater range of variation for D-DS ($-0.04 < \Delta\gamma_r(t) < 0.02$). For CLDV and OPDV points, the distribution of $\Delta\gamma_r$ in the three environments have also been compared using the Kolmogorov-Smirnov test. Of course, for a full comparison, distributions have been normalised with respect to the maximum value or the minimum one (respectively for OPDV and CLDV). As a result six distributions between 0 and 1 have been obtained. The test showed that the two simulated environments are not significantly different (with p-values of 0.63 with reference to CLDV, and 0.06 with reference to OPDV). With reference to the IV, both the environment are significantly different (all the tests gave p-values lower than 0.001).

4 Summary

The possibility to observe variables directly correlated to drivers' actions, such as gas pedal pressure, allows an in-depth discussion concerning action point paradigms. In the case of points OPDV and CLDV the behaviour of drivers was shown to change rather sharply. In particular, before CLDV a reduction in pedal

pressure is observed, while an increase can be associated to OPDV. By contrast, small variations were observed at points ABX and SDX, where respectively a local minimum and maximum mean value is observed, even though around the t_{ap} instants (e.g. t_{ap} -1, t_{ap} +1) these values tend to be ordered like those of a *flat function* (see Figures 5, 8 and 11). Importantly, the existence of ABX and SDX is specific to Wiedemann's model, while it is neglected in previous approaches, where the applied pedal pressure (and the relative acceleration) are considered constant between CLDVs and OPDVs. The results of our study seem to confirm the approach adopted by Todosoiev and Barbosa. Alternatively, a particular case of Wiedemann's paradigm, as described by Figure 6, could have occurred, where some F_SDX (False SDX) and F_ABX (False ABX) points were selected as candidate APs as a consequence of the AP selection algorithm, which is based on purely kinematic conditions. However, these points do not correspond to any actual action and are only the direct consequence of actions previously taken at OPDV or CLDV. Further confirmation can be found in the recent work of Bifulco et al. (2013), even if obtained without direct observation of pedal actions, where ABX and SDX are identified as only pass-through points (with no behavioural relevance), and where a linear pattern is found to fit (in what is called an *opening chart*) the observed CLDV and OPDV points using the inverse of TTC. Also Hoogendoorn et al. (2011), using empirical data, identified action points by analysing accelerations, and stored, once a point was classified as an action point, the spacing and relative speed at the detection instants. Using these points, they defined some regions in the phase-plane in which the driver is likely to perform an action (in the sense that he/she is likely to decrease or increase acceleration). Once again, patterns very similar to CLDV and OPDV curves were obtained, while patterns for ABX and SDX were not detected.

Interestingly, the proposed curves were calibrated using spacing and relative speed conditions at the detection instants, while it was shown that the actual action by the driver starts several instants before (see Figures 5, 7 and 12), and thus the stimulus that determines the action starts even before . In particular, the pedal operations start (and finish) in different instants (with reference to t_{ap}), and last the same time for the S-DS and the IV (1.6 seconds for closing actions, 2.4 seconds for opening actions), while they are shorter (1 second for closing actions, 1.6 seconds for opening actions) in the D-DS environment. These lags should be considered in the calibration of CLDV and OPDV thresholds. Indeed, stimuli should be sought where the actions are actually performed (or even before, considering the perception-reaction time), and a *pedal-based* calibration procedure could be applied. As an alternative, the kinematic-based calibration should carefully take into account anticipation with respect to t_{ap}. In any event, a pedal-based procedure like that applied in this work, possibly associated with a disaggregate analysis, has the potential to give a conclusive explanation of the AP paradigm.

The observed data evidence an asymmetric behaviour in terms of acceleration/deceleration applied, as both the magnitude and the duration of the action at closing (CLDV) and opening (OPDV) phases are different. This asymmetric behaviour confirms the findings by Forbes (1963) who noticed that the driver's response is slower in acceleration than in deceleration. This represents an interesting issue that has consequences in traffic flow phenomena as well. For instance, Newell (1965) suggested that, for the same speed, the applied spacing in acceleration manoeuvres always exceeds that in deceleration. What is important is that this asymmetry produces *clockwise loops* in the flow-density plane, later referred to as the *traffic hysteresis phenomenon* (Treiterer and Myers, 1974). Studies related to this phenomenon as well as to its effect on the traffic stream still represent an open question, as demonstrated by the recent work by Yeo (2008).

A final issue concerns observed patterns of the variables considered in the three environments which, albeit differing in magnitude, become very similar (and consistent with literature) once scaled properly, that is by normalising with respect to absolute values ($\Delta\gamma_r$) and by accepting different duration of the actions. It is worth noting that although we retain equivalent the observed phenomena from a qualitative

point of view, quantitative differences exist. However, authors' opinion is that differences between experimental environments are not a matter of drivers behaving differently. Rather, they depend on different dynamics (especially inertia) of the three vehicles involved in the experiment, on one hand the IV and on the other hand the two virtual cars, modelled in the two different DS environments. Of course the two virtual cars are similar because of the same adopted driving simulation software and the same parameters for characterising the virtual car. In the context of our analyses the previous considerations are not a matter, as the observed phenomena are qualitatively similar in the different contexts (virtual and naturalistic). However, our analyses show that driving simulators are validated environment for driving behaviour (car-following) studies only in terms of relative validations. Observation and comparison techniques (as the ones adopted in this paper) could be applied in the future in order to check (and tune) for full validation of virtual driving environments.

5 Conclusions

The work described in this paper was based on a large-scale experimental campaign carried out in Italy during the DriveIn[2] research project. The campaign involved 100 drivers who experienced the same scenario in both a real and virtual environment, with each driving session lasting about one hour. Data were analysed in the framework of the Action Point theory, and on the basis of kinematic conditions different kinds of candidate APs (according to Wiedemann's definition) were selected and classified. The total number of selected candidate APs exceeded 29,000 points. Analyses have been carried out in order to further investigate candidate APs with the aim to check for actual APs. Candidate APs were analysed with reference to the use of the gas pedal, employed by drivers to control the vehicle in close-following conditions. The results show that actual actions can be associated to candidate action points defined with respect to relative velocity (CLDV and OPDV). The aggregate analysis of the candidate points defined with respect to space (ABX and SDX) does not support the evidence that actual actions can be systematically associated to these points.

Our results support the implementation of simpler theories (e.g. calibration of two AP thresholds instead of four). This is particularly relevant to Advanced Driving Assistance Systems, where the solutions based on the reproduction of driving behaviour have to be applied on line, with evident performance/efficiency requirements.

Future research efforts in the field explored by this work could involve analysing the distribution of (actual) APs among drivers, and possible clustering of drivers with similar behaviour (and comparison of the resulting clusters with those resulting from psychological measures).

6 Acknowledgments

The authors would like to thank the anonymous reviewers for their helpful comments. Data used in this work were supplied by the PON (Programma Operativo Nazionale) 2007–2013 – Research Project B61H110004000005 (DRIVE IN2). Analyses and developments ware partially supported within the PON Research Project B68F12001150005 (App4Safety).

References

Alexiadis, V., Colyar, J., Halkias, J., Hranac, R. and McHale, G. (2004) The next generation simulation program, *ITE Journal (Institute of Transportation Engineers)*, vol. 74(8), 22-26.

Barbosa, L. (1961) Studies on Traffic Flow Models. Reports No. 202A-1. The Ohio State University Antenna Laboratory

Bham, G.H. and Benekohal, R.F. (2004) A high fidelity traffic simulation model based on cellular automata and car-following concepts. *Transportation Research Part C: Emerging Technologies*, vol. 12(1), 1-32.

Bifulco, G.N., Pariota, L., Simonelli, F. and Di Pace, R. (2011) Real time smoothing of car-following data through sensor fusion techniques, *Procedia - Social and Behavioral Sciences*, vol. 20, 524-535.

Bifulco, G.N., Pariota, L., Galante, F., and Fiorentino, A. (2012). Coupling instrumented vehicles and driving simulators: opportunities from the DRIVE IN2 project. 15th International IEEE Conference on Intelligent Transportation Systems (ITSC), Anchorage (AK, USA), Sept. 16-19, article no. 6338789, pp. 1815-1829.

Bifulco, G.N., Pariota, L., Brackstone, M. and McDonald, M. (2013) Driving behaviour models enhancing the simulation of Advanced Driving Assistance Systems: revisiting the Action Point paradigm, *Transportation Research Part C: Emerging Technologies*, vol. 36, 352-366.

Boer, E..R. (1999) Car-following from the driver's perspective, *Transportation Research Part F: Traffic Psychology and Behaviour*, 2(4), 201-206.

Brackstone, M., Sultan, B. and McDonald, M. (2002) Motorway driver behaviour: studies on car following. *Transportation Research Part F: Traffic Psychology and Behaviour, vol.* 5**,** 31-46.

Colombaroni, C., and Fusco, G. (2014) Artificial neural network models for car following: Experimental analysis and calibration issues. *Journal of Intelligent Transportation System*, vol. 18(1), 5-16.

Fancher, P., S. and Bareket, Z. (1998) Evolving model for studying driver-vehicle system performance in longitudinal control of headway. *Transportation Research Record*, vol. 1631, 13-19.

Forbes, T.W. (1963) Human factor consideration in traffic flow theory. *Highway Research Record*, 15, pp. 60–66

Fritzsche, H-T. (1994). A model for traffic simulation. *Transportation Engineering Contribution,* vol. 5, 317–321.

Gazis, R., Herman, R. and Rothery, R., W. (1961). Nonlinear follow the leader models of traffic flow. *Operations Research*, vol. 9, 545-567.

Gipps, P., G. (1981) A behavioural car-following model for computer simulation. *Transportation Research Part B: Methodological, vol.* 15**,** 105-111

Hoffmann, E., R. and Mortimer, R., G. (1996). Scaling of relative velocity between vehicles. *Accident Analysis and Prevention*, vol. 28 (4), 415-421.

Hoogendoorn, S., P., and Ossen, S. (2006) Empirical Analysis of Two-Leader Car-Following Behavior, *European Journal of Transport and Infrastructure Research*, vol. 6(3), 229-246.

Hoogendoorn, S., P., Hoogendoorn, R., G. and Daamen, W. (2011). Wiedemann Revisited: New Trajectory Filtering Technique and Its Implications for Car-Following Modeling. *Transportation Research Record: Journal of the Transportation Research Board*, vol. 2260, 152-162.

Kikuchi, P. and Chakroborty, P. (1992) Car-following model based on fuzzy inference system. *Transportation Research Record: Journal of the Transportation Research Board*, vol. 1365(1992), 82-91.

Michaels, R.M. (1963). Perceptual factors in car following. In *Proceedings of the Second International Symposium on the Theory of Road Traffic Flow,* 44‑59. Paris: OECD

Montroll, E.W. (1959). Acceleration and clustering tendency of vehicular traffic. In *Proceedings of the Symposium on Theory of Traffic Flow*, Research Laboratories, General Motors 147‑157. New York: Elsevier

Newell, G.F., (1965). Instability in dense highway traffic, a review. In: Proceedings of the Second International Symposium on The Theory of Road Traffic Flow, London, pp. 73–83.

Pariota L, Bifulco L, Brackstone M (2015, on-line pub.) A linear dynamic model for driving behaviour in car-following. *Transportation Science* (articles in advance), doi: 10.1287/trsc.2015.0622

PTV-AG, VISSIM 5.10 User Manual. 2008

Saifuzzaman, M., and Zheng, Z. (2014) Incorporating human-factors in car-following models: A review of recent development and research needs. *Transportation Research Part C: Emerging Technologies*, vol. 48, 379-403

Todosoiev, E., P. (1963) The Action Point Model of the Driver Vehicle System. Report No. 202A-3. The Ohio State University, Engineering Experiment Station, Columbus, Ohio.

Treiber, M., Hennecke, A., Helbing, D. (2000) Congested traffic states and anticipation in microscopic traffic models. *Physical Review E*, vol. 62(2), 1805-1824.

Treiterer, J., Myers, J.A., (1974). The hysteresis phenomenon in traffic flow. In: Proceedings of the Sixth International Symposium on Transportation and Traffic Theory, Sydney, Australia, pp. 13–38.

Wagner, P. (2011). A time-discrete harmonic oscillator model of human car-following. *European Physical Journal B*, 84 (4), 713-718.

Wiedemann, R. (1974) Simulation des Strassenverkehrsflusses Tech. Rep. Institut für Verkehrswesen. Universität Karlsruhe, Heft 8 der Schriftenreihe des IfV (in German).

Yeo, H., 2008. Asymmetric Microscopic Driving Behavior Theory. Ph.D. thesis, University of California.

Zgonnikov, A. and Lubashevsky, I. 2014 Extended phase space description of human-controlled systems dynamics. *Progress of Theoretical and Experimental Physics*, vol. 3, 033J02

Table

Table I – Action points, expected dynamics and expected action in Wiedemann's theory

Point/*Phase*	**Description**	**Expected Dynamics**	**Expected Action**
Free-flow Phase	*Given Δv, the spacing Δx is very large. Hence $d\vartheta/dt$ is negligible and the driver does not perceive any stimulus*	*The follower cruises at the desired speed and unconsciously approaches the leader. The spacing progressively decreases and thus $d\vartheta/dt$ increases toward non-negligible values*	
SDV Point	The spacing Δx, starting from far away, has reached a threshold (SDV) such that (given the relative speed Δv) the angular velocity ($d\square/dt$) is perceived and stimulates the driver	The follower starts changing the dynamics of the vehicle from uniform speed to (constant) deceleration.	The gas pedal is relaxed
Consciously Approaching Phase	*Both the relative speed (in absolute value) and the spacing progressively decrease, the angular velocity ($d\vartheta/dt$) tends to be constant and the driver is not stimulated*	*The relative speed (Δv) is still negative but is going to progressively decrease in absolute value; the spacing decreases too*	
ABX Point	The relative speed Δv is very low (in absolute value), but the spacing Δx has reached a threshold value (ABX) and the angular velocity $d\square/dt$ stimulates the driver to further slow down in order to keep the spacing required for controlling the vehicle	A further deceleration is started, in addition to that already applied (constant)	The gas pedal is further relaxed (or the brake is slightly pushed down)
Opening Phase	*The relative speed Δv is positive and still small in absolute value and the spacing increases. The angular velocity $d\vartheta/dt$ is small and does not stimulate the driver*	*Both the relative speed and the spacing increase*	
OPDV Point	The relative speed Δv has reached a threshold value (OPDV) and is enough to produce a stimulating angular velocity $d\square/dt$	The follower starts to apply the transition from a (constant) deceleration to a (constant) acceleration, in order to start closing the gap	The gas pedal is pushed down
Still Opening (but actually with closing intention) Phase	*The relative speed Δv decreases and the spacing Δx increases; there is no stimulus from the angular velocity $d\vartheta/dt$*	*The gap is still opening but with a reduced gradient, according to the closing intention at OPDV*	
SDX Point	The relative speed Δv is very low (in absolute value), but the spacing Δx has reached a threshold value (SDX) such that the contact seems to be lost with the leading vehicle;	A further acceleration is started, in addition to that already applied (constant)	The gas pedal is further pushed down
Closing Phase	*The relative speed Δv is negative and increasing in absolute value, the spacing Δx decreases; the angular velocity $d\vartheta/dt$ progressively increases*	*The gap is closing*	
CLDV	The (negative) relative speed Δv has reached a threshold value (CLDV) and is high enough to produce a stimulating angular velocity $d\square/dt$	The follower starts to apply the transition from a (constant) acceleration to a (constant) deceleration, in order to start opening the gap	The gas pedal is relaxed (or the brake pushed down)
Still closing (but actually with opening intention) Phase	*The (negative) relative speed Δv decreases in absolute value and the spacing Δx also decreases; there is no stimulus from the angular velocity $d\vartheta/dt$*	*The gap is still closing but with a reduced gradient, according to the opening intention at CLDV*	
ABX point again	The conditions for the ABX point hold again and the unconscious car-following phase goes on periodically		

Table II –Number of drivers involved, sections selected and candidate APs detected, per experimental environment

	Involved Drivers	***Sections***					***Detected Candidate APs***			
		Total Number	*Length [km]*		*Duration [min]*		*CLDV*	*ABX*	*OPDV*	*SDX*
			total	*mean (st.dv.)*	*total*	*mean (st.dv.)*				
S-DS	99	2670	2964	1.11 (1.90)	1968	0.74 (1.20)	3003	3003	2859	2859
D-DS	22	290	768	2.65 (2.51)	570	1.97 (1.36)	980	980	1006	1006
IV	100	1279	2303	1.80 (1.96)	1664	1.30 (1.32)	3274	3274	3367	3367

The number of CLDV and ABX (as well as the number of OPDV and SDX) in each environment is the same as a consequence of the AP detection algorithm.

Figure

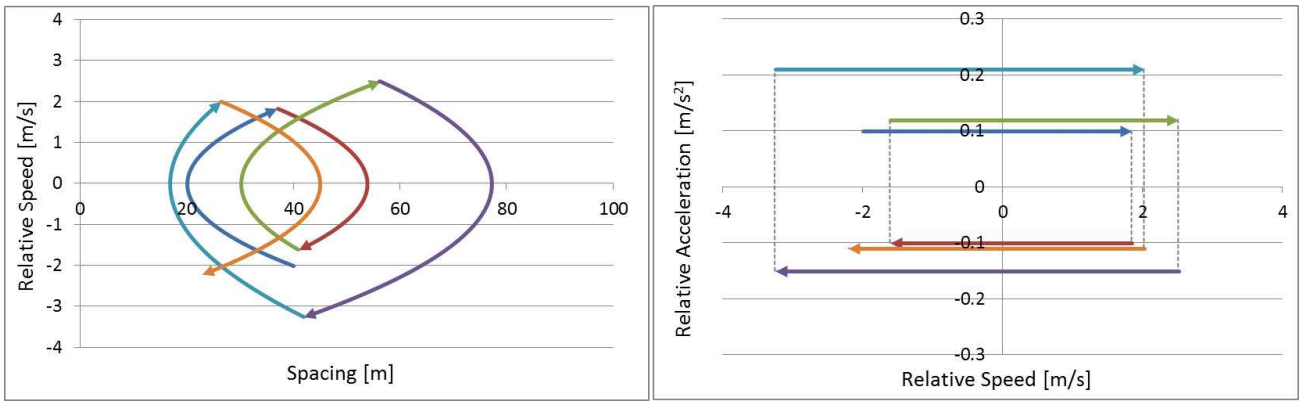

Figure 1 - An example of phase planes (left: first-order; right: second-order)

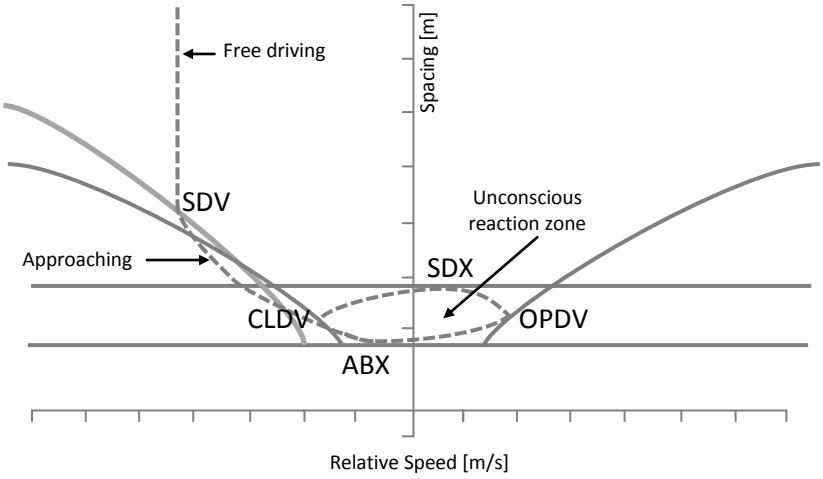

Figure 2 – Graphical representation of Wiedemann's paradigm – The relative speed has opposite direction with respect to the original paper

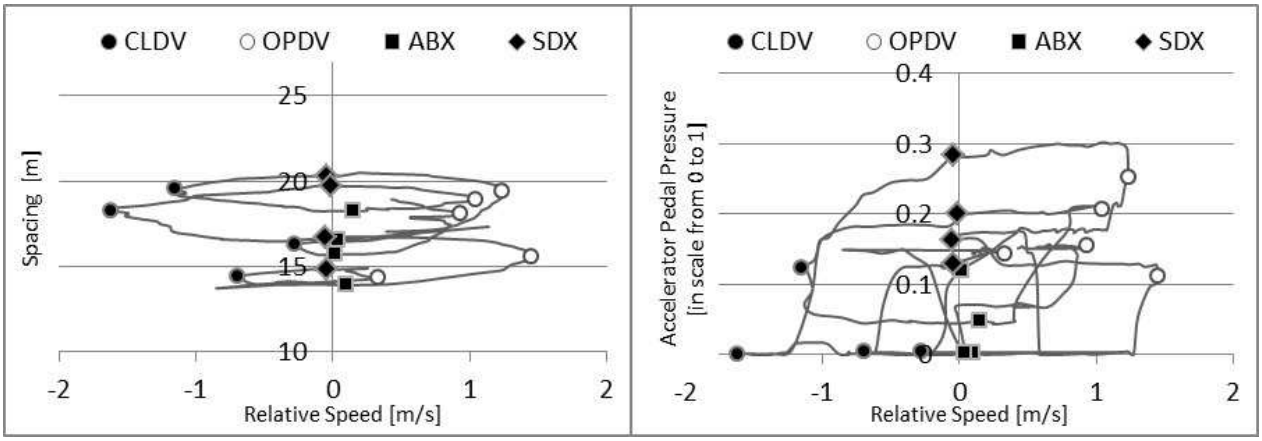

Figure 3 – Typical experimental car following spirals, with APs evaluated in accordance with Wiedemann's paradigm, depicted in the Spacing vs. Relative Speed plane (left), and in terms of gas-pedal pressure (right). Ground velocity around 70 km/h, observation time 30 seconds.

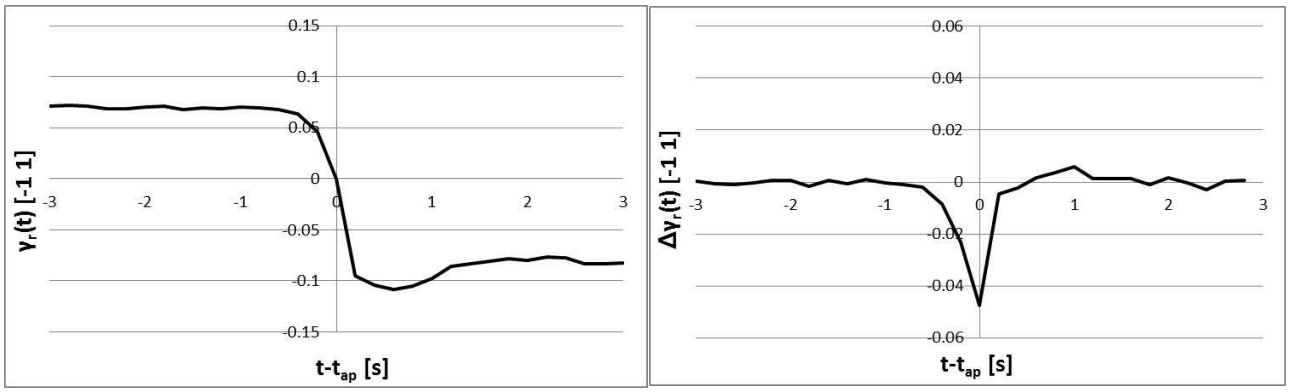

Figure 4 – The values of $\gamma_r(t)$ variables around a CLDV point (left), and the associated $\Delta\gamma_r(t)$ pattern (right).

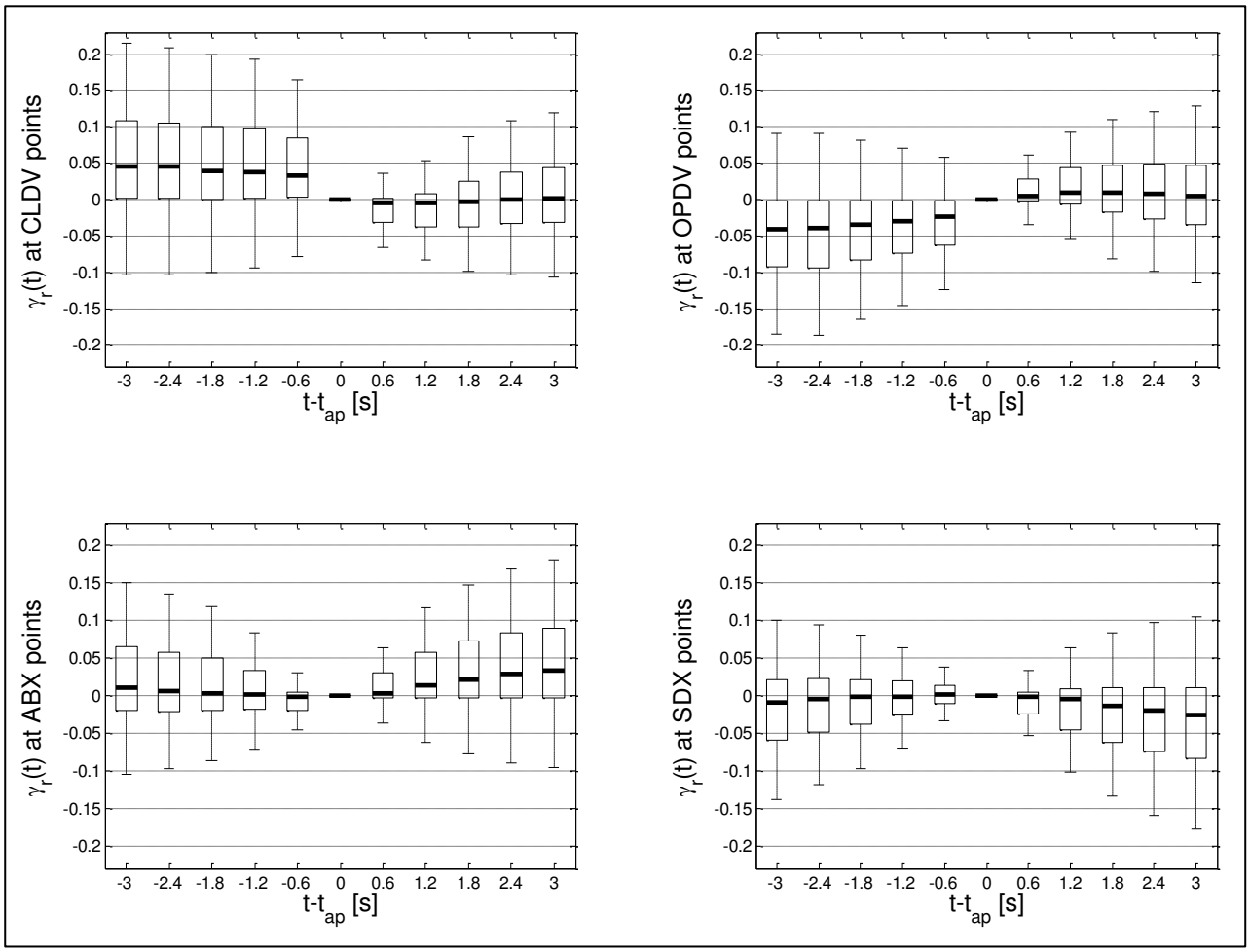

Figure 5 – The values of $\gamma_r(t_{ap})$ at the four candidate APs; boxes represent respectively first, second (in bold) and third quartiles of the distribution, whiskers show 95% coverage of the data.

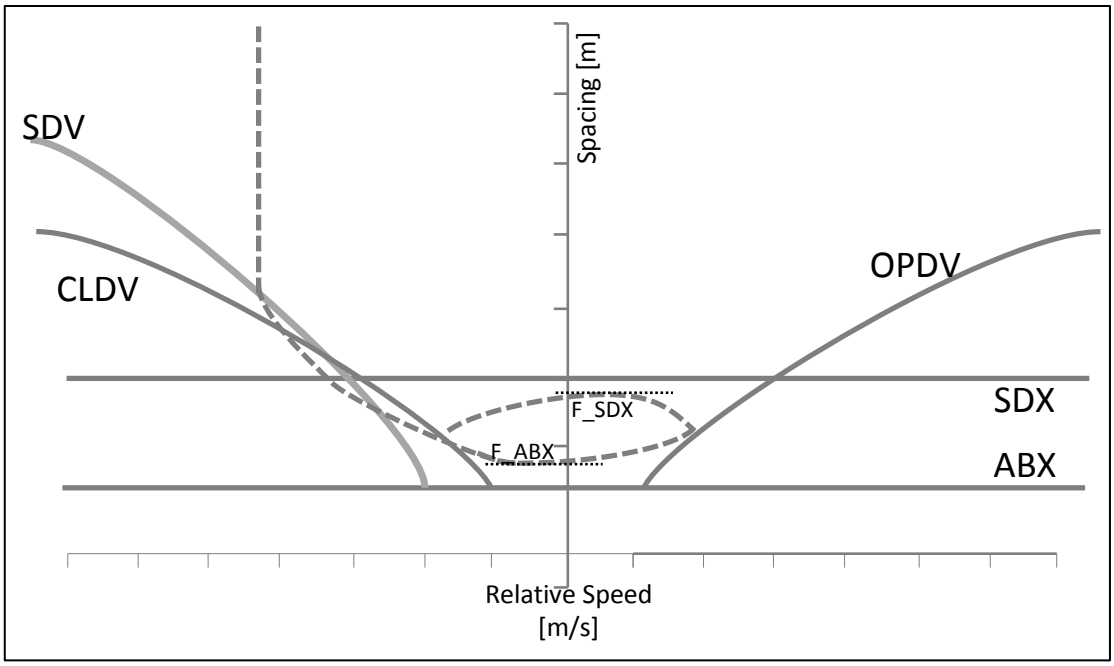

Figure 6 – The particular case in Wiedemann's paradigm evidenced in the discussed data– The relative speed has opposite direction with respect to the original paper

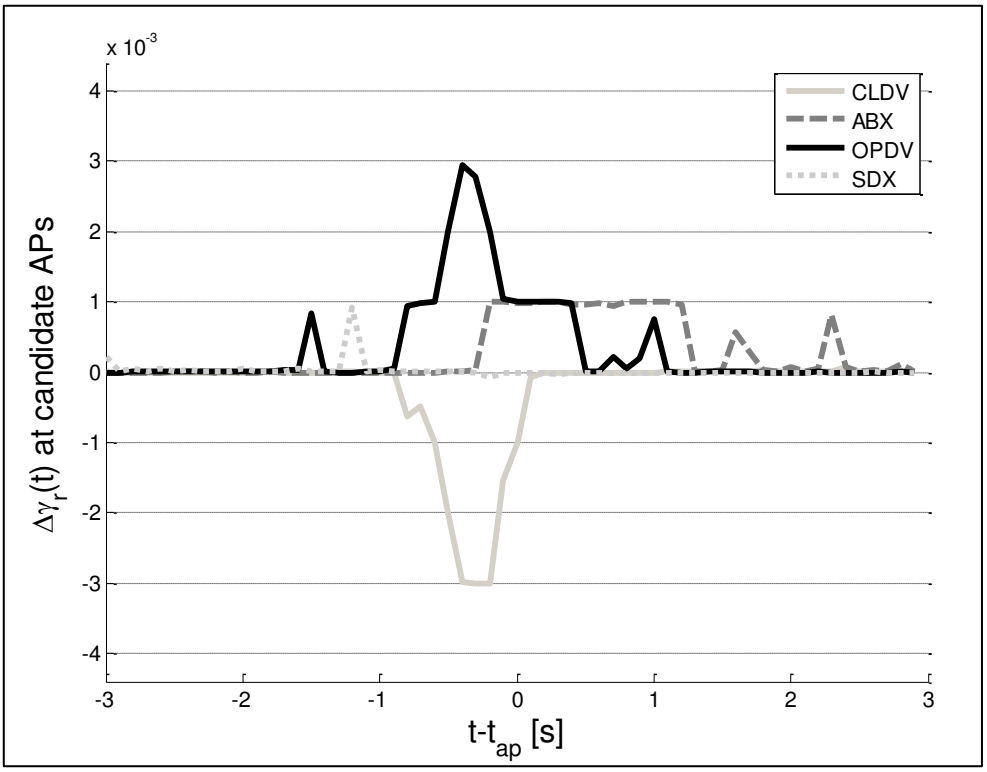

Figure 7 – The distribution of the $\Delta\gamma_r(t)$ median values around all the potential APs (Δt=0.1 s)

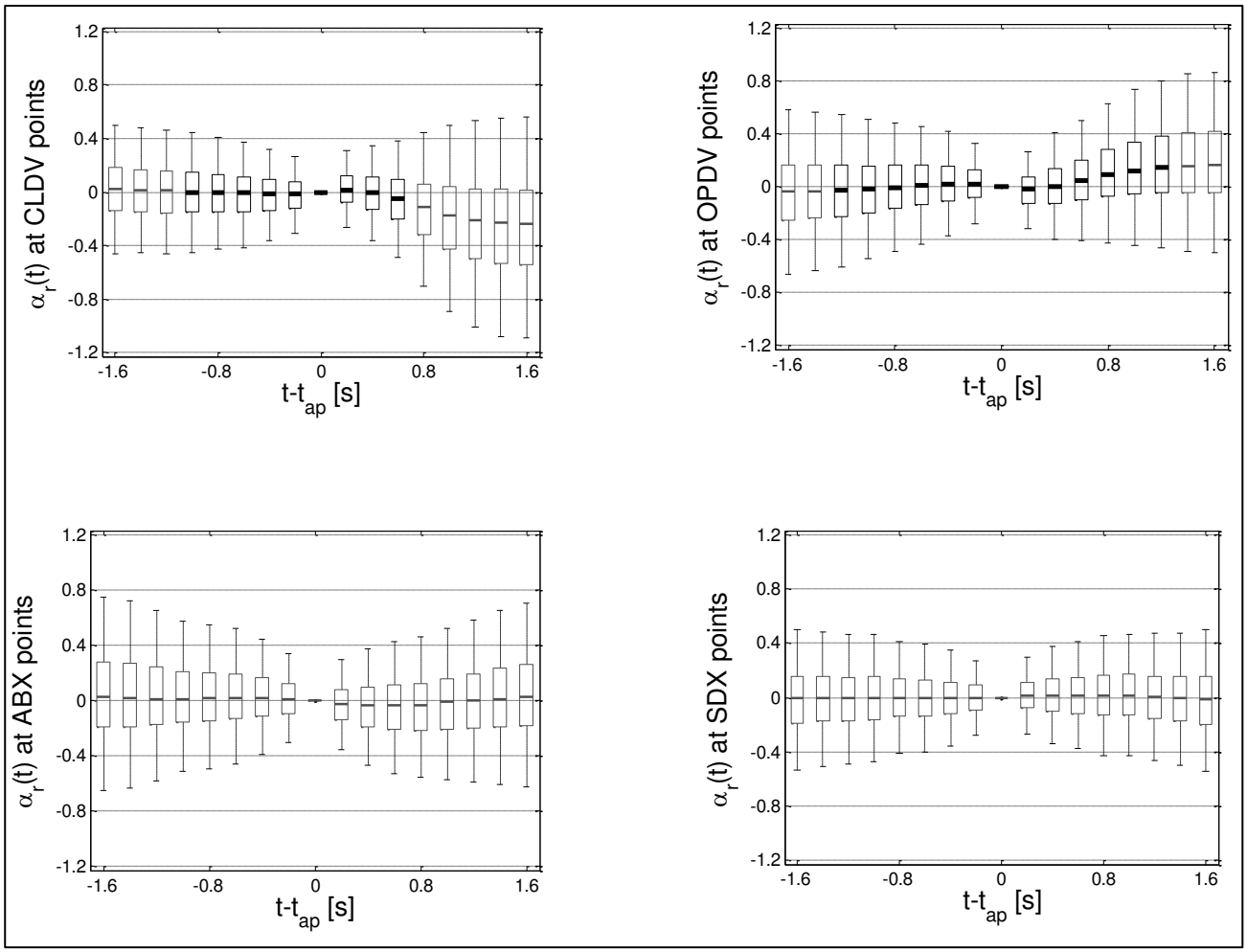

Figure 8 –Statistical distributions of $\alpha_r(t)$, observed with the instrumented vehicle; boxes represent respectively first, second and third quartiles of the distribution, whiskers show 95% coverage of the data. For CLDV and OPDV points, accelerations concerning time-intervals obtained from the analysis of $\Delta\gamma_r(t)$ are depicted in bold.

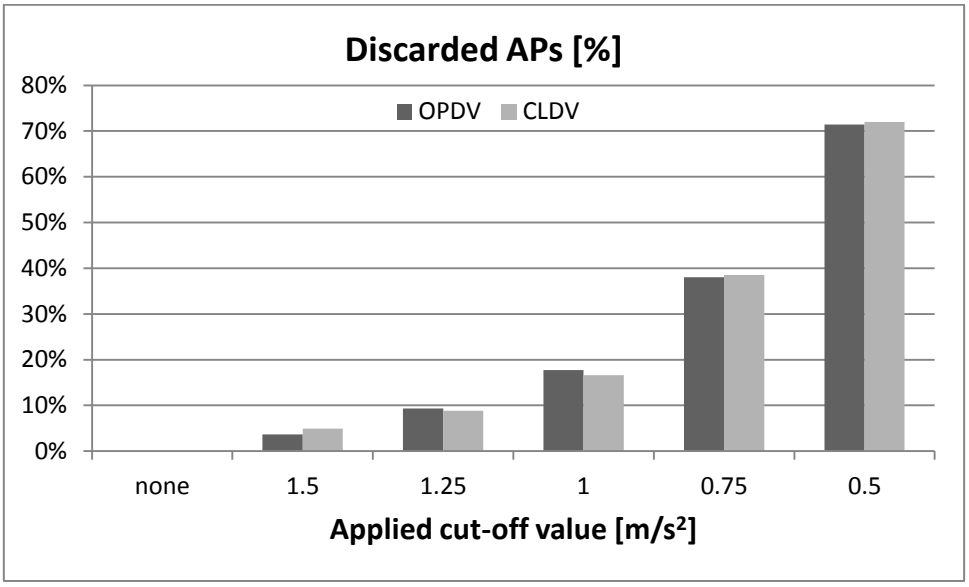

Figure 9 – Number of APs discarded from the analysis with different thresholds for accepted α(t); patterns are shown for no-threshold and cut-off values of 1.5, 1.25, 1, 0.75 and 0.5 m/s²

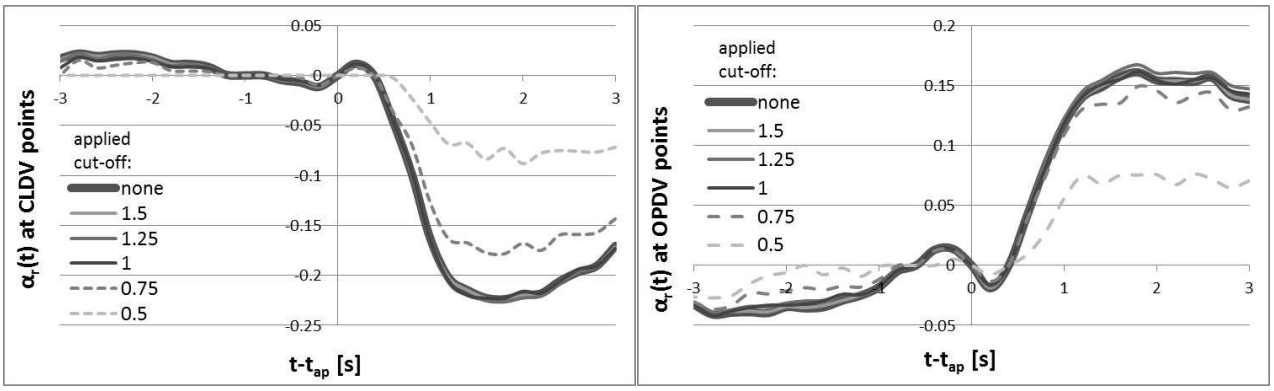

Figure 10 – The distribution of the median values of $\alpha_r(t)$ with different thresholds for accepted $\alpha(t)$; patterns are shown for no-threshold and cut-off values of 1.5, 1.25, 1, 0.75 and 0.5 m/s^2

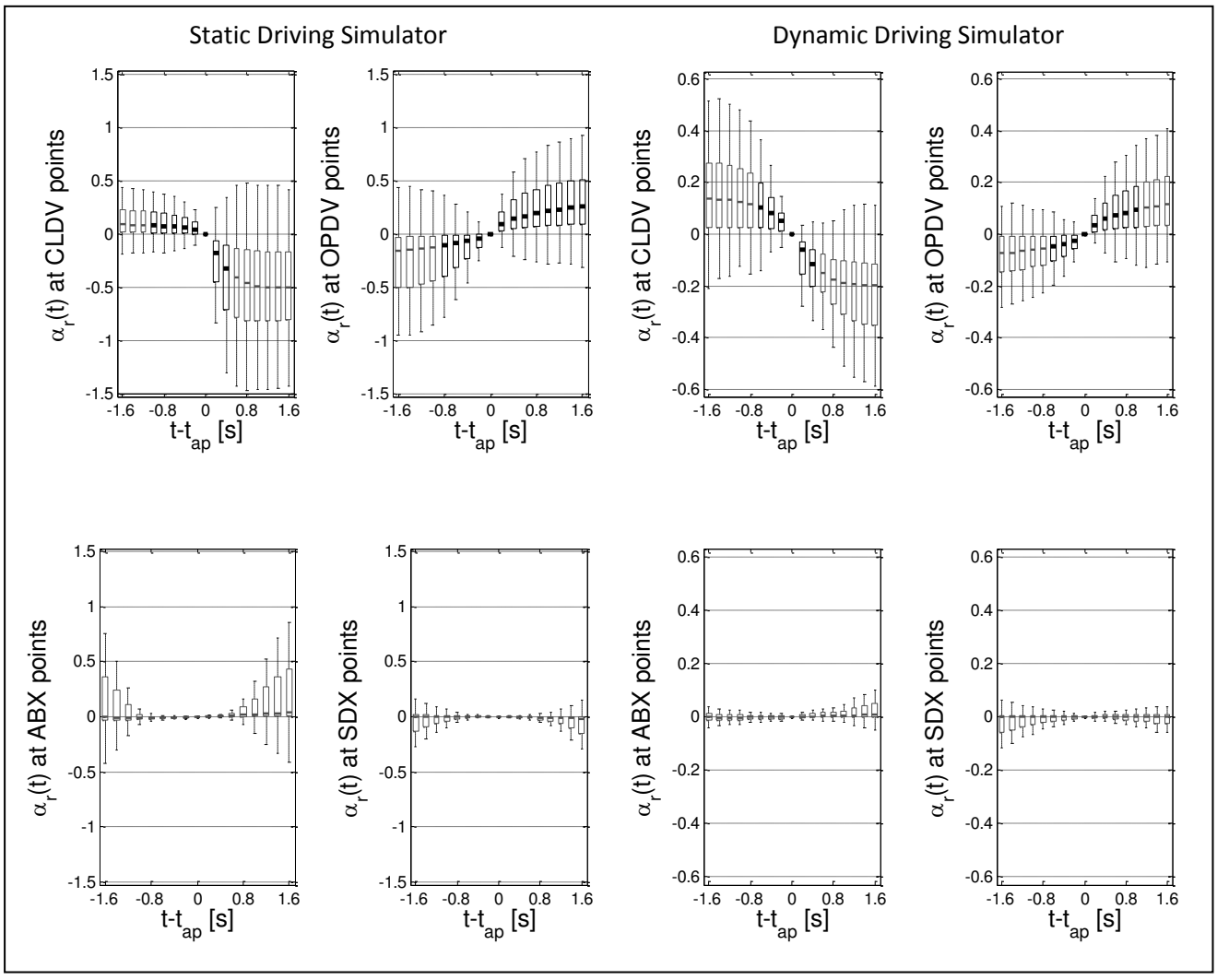

Figure 11 –Statistical distributions of $\alpha_r(t)$ at driving simulators; boxes represent respectively first, second and third quartiles of the distribution, whiskers show 95% coverage of the data. For CLDV and OPDV points, accelerations concerning time-intervals obtained from the analysis of $\Delta\gamma_r(t)$ are depicted in bold.

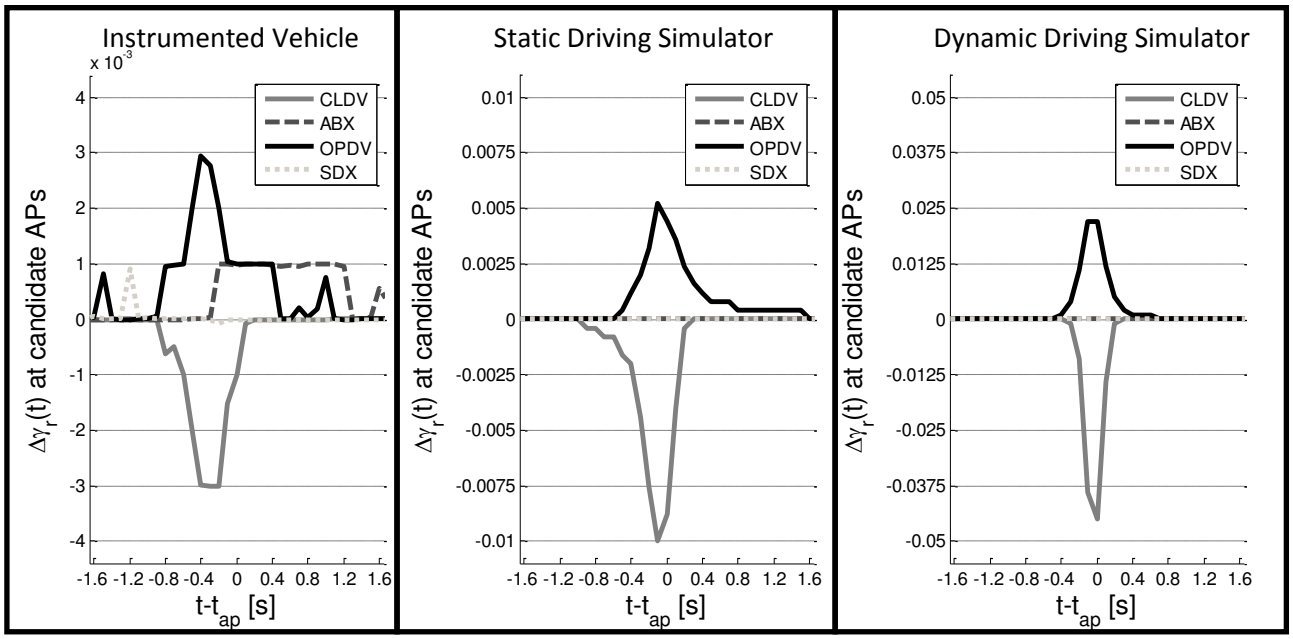

Figure 12 – The distribution of the $\Delta\gamma_r(t)$ median values around all the potential APs (Δt=0.1 s) in the three experimental environments